



# An interdisciplinary approach to the study of kiln firing: a case study from the Campus Galli open-air museum (southern Germany)

Silvia Amicone<sup>1,2</sup> · Alisa Memmesheimer<sup>1</sup> · Baptiste Solard<sup>1</sup> · Shira Gur-Arieh<sup>3,4</sup> · Martin Rogier<sup>5</sup> · Awais Mohammed Qarni<sup>1</sup> · Johannes Seidler<sup>1</sup> · Paola Sconzo<sup>6</sup> · Lars Heinze<sup>7</sup> · Lionello F. Morandi<sup>1,8</sup> · Tobias Kiemle<sup>1</sup> · Christopher E. Miller<sup>9,10</sup> · Klaus G. Nickel<sup>1</sup> · Christoph Berthold<sup>1</sup>

Received: 11 November 2022 / Accepted: 25 May 2023 / Published online: 10 July 2023  
© The Author(s) 2023

## Abstract

Pottery kilns are a common feature in the archaeological record of different periods. However, these pyrotechnological installations are still seldom the target of interdisciplinary investigations. To fill this gap in our knowledge, an updraft kiln firing experiment was run at the Campus Galli open-air museum (southern Germany) by a team consisting of experimental archaeologists, material scientists, geoarchaeologists, and palaeobotanists. The entire process from the preparation of the raw materials to the firing and opening of the kiln was carefully recorded with a particular focus on the study of the raw materials used for pottery making, as well as on fuel usage. The temperatures were monitored by thermocouples placed at different positions in the combustion and firing chambers. In addition, thermocouples were installed within the kiln wall to measure the temperature distribution inside the structure itself. Unfired raw materials as well as controlled and experimentally thermally altered ceramic samples were then characterised with an integrated analysis including ceramic petrography, X-ray diffraction (XRD), Fourier transform infrared spectroscopy (FTIR), scanning electron microscopy (SEM), and portable X-ray fluorescence (pXRF). Our work provides data about mineralogical and microstructural developments in both pottery kiln structures and the ceramics produced in this type of installations. This is helpful to discuss the limits and potential of various scientific analyses commonly used in ancient ceramic pyrotechnological studies. Overall, our work contributes to a better understanding of updraft kiln technology and offers guidelines on how to address the study of this type of pyrotechnological installations using interdisciplinary research strategies.

**Keywords** Updraft kiln · Pyrotechnology · Pottery · Experimental archaeology

✉ Silvia Amicone  
silvia.amicone@uni-tuebingen.de

<sup>1</sup> Archaeometry Research Group, Competence Center Archaeometry – Baden-Wuerttemberg, University of Tübingen, Tübingen, Germany

<sup>2</sup> Institute of Archaeology, University College London, London, UK

<sup>3</sup> The Leon Recanati Institute for Maritime Studies, University of Haifa, Haifa, Israel

<sup>4</sup> Institute for Pre- and Protohistoric Archaeology and Archaeology of the Roman Provinces, Ludwig Maximilian University of Munich, Munich, Germany

<sup>5</sup> Campus Galli, Meßkirch, Germany

<sup>6</sup> Dipartimento di Culture e Società, University of Palermo, Palermo, Italy

<sup>7</sup> Archaeological Institute, University of Cologne, Cologne, Germany

<sup>8</sup> Dipartimento di Civiltà e Forme del Sapere, University of Pisa, Pisa, Italy

<sup>9</sup> Institute for Archaeological Sciences and Senckenberg Centre for Human Evolution and Palaeoenvironment, University of Tübingen, Tübingen, Germany

<sup>10</sup> SFF Centre for Early Sapiens Behaviour (SapienCE), University of Bergen, Bergen, Norway

## Introduction

Ceramic pyrotechnology has come into focus through several works that illustrate the complexity of this procedure as long with its wider implications for the study of invention, innovation, and technological advancement in the ancient world (e.g. Gibbs 2015; Gosselain 1992; Livingstone Smith 2001; McDonnell 2001; Rice 2015; Wertime 1964).

Archaeometric analysis has been crucial amongst the different approaches that have been used to reconstruct ancient ceramic pyrotechnology (e.g. Gliozzo 2020; Tite 1995 and literature therein). These studies employ a variety of methods aimed to reconstruct the firing process with a particular focus on the estimation of maximum firing temperatures. More precisely, these methods are based on studies that established clear relationships between parameters of firing procedures, such as temperature and atmosphere with changes in the pottery microstructure (e.g. porosity, clay matrix, progressive sintering, vitrification) and mineralogy (e.g. Gliozzo 2020; Heimann and Maggetti 2019; Kazakou et al. 2019; Maniatis and Tite 1981; Maritan et al. 2006, 2007; Rice 2015, pp. 376–387).

Another major focus of pyrotechnological studies are ancient combustion features such as pottery kilns, whose study has enormous potential to gain better insights into a variety of other aspects of the dynamics of kiln firings, such as the degree of insulation, separation of fuel and vessels, and heating and cooling rates, as well as soaking times and fuel usage (Thér et al. 2019). Pyrotechnological installations for pottery firing are a common feature of many archaeological sites, and there are several studies regarding their morphology (e.g. Cuomo di Caprio 1972; Delcroix and Huot 1972; Dufay 1996; Duhamel 1974; Hansen Streily 2000; Hasaki 2002; Swan 1984), in addition to experimental works that try to test hypotheses on their use and performances (e.g. Hanning et al. 2016; Maggetti et al. 2011; Thér 2014).

However, kilns are rarely targeted for systematic and multi-disciplinary investigations. Recent studies have shown the potential of combining archaeometric with geoarchaeological approaches to reconstruct the life history of these pyrotechnological installations and to acquire more information about their use (Karkanias et al. 2019; Squitieri et al. 2022; Weiner et al. 2020).

Nevertheless, studies that have combined both experimental works in the laboratory and in the field with systematic programmes of scientific analysis are still scant (e.g. Maggetti et al. 2011; Thér et al. 2019). Such an approach has the potential to provide more precise data on different aspects of firing procedures and how these are reflected in the microstructural and compositional characteristics of ceramics.

This data can improve interpretation of instrumental measurements and help us to develop a more detailed technological and social reconstruction of ancient ceramic pyrotechnology (e.g. Amicone et al. 2021). In this paper, we present the results of an experiment run on an updraft kiln built in the Campus Galli open-air museum (Meßkirch, southern Germany). We chose to run this experiment using this type of kiln, as it is one of the most common firing installations in the archaeological record found in different parts of the world across different chronological periods (Roux 2019). The aim of the experiment was to collect data on updraft kiln firing procedures along with information about microstructural developments in both the kiln structure and the sintered ceramics produced in it. A variety of scientific methods were undertaken on fired ceramic samples collected during the experiment, as well as from the kiln walls. Our work contributes to understanding one of the most common types of firing installation of the ancient world, providing new data which enhances the interpretation of current and future analyses of a variety of archaeological analogues on a broad spatial and temporal scale.

Furthermore, our paper discusses how to improve research strategies such as sampling and analytical methods for these types installations by integrating experimental archaeology and natural science approaches.

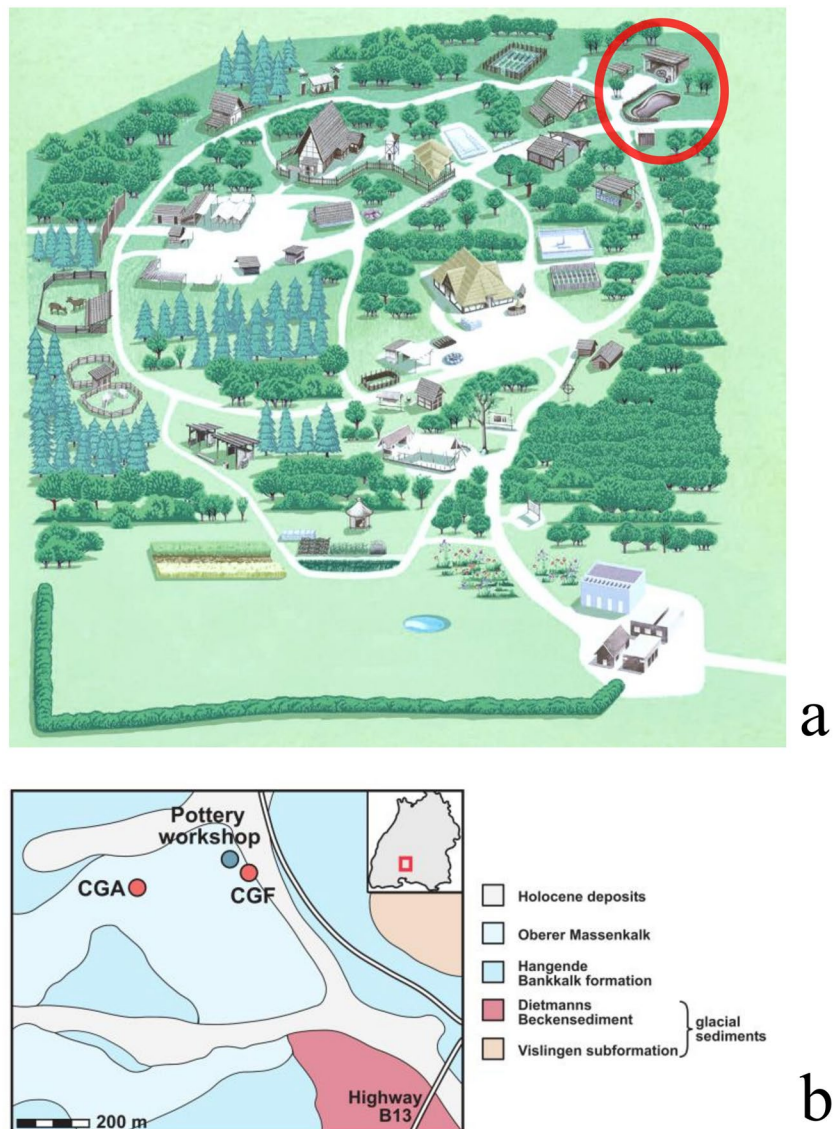
### The Campus Galli open-air museum and its pottery workshop

The open-air museum of Campus Galli (Fig. 1a) is a construction site where an early mediaeval monastery is currently being built according to the so-called Plan of St. Gall, an architectural drawing from the first half of the ninth century AD (Carolingian period) (Schedl 2014; Tremp 2014).

Compared to many other archaeological open-air museums, its focus is not only on reconstructing past buildings, but also on offering a space where building techniques and various crafts, as well as daily life activities, could be re-enacted. In 2018, the Competence Center Archaeometry – Baden-Wuerttemberg of the University of Tübingen began a collaboration with Campus Galli to promote research and teaching activities on ancient crafts involving the local community, students, and various scientists. One of the core craft activities present in Campus Galli is the production of pottery. Martin Rogier established a potter's workshop which includes facilities for extraction and processing of raw materials and water basins to levigate the clay, as well as a potter's wheel along with an updraft kiln, both built according to mediaeval models (Rogier 2018).

Updraft kilns consist of different parts: a fire tunnel or heat channel from where the fuel is loaded; the combustion chamber or firebox where fuel is placed to burn; the firing chamber,

**Fig. 1** **a** Map of the Campus Galli open-air museum, Baden-Württemberg, Germany. Pottery workshop located in red circle (<https://www.campus-galli.de>); **b** Simplified geological map of the area around the pottery workshop (Lars Heinze)



also called stack area, where the pots are set to be fired over the kiln floor; and the exit flue at the top of the kiln from where the potter can control the kiln's atmosphere. This is one of the most diffused types of kilns of the ancient world and is still in use amongst traditional communities of potters today. In this type of installation, the flame is introduced into the bottom of the kiln, at or below floor level, and exhausted out the top.

The updraft kiln (Fig. 2) used in this experiment was built in 2016 to early mediaeval design (Rogier 2018); however, it showcases an architecture which is consistently seen across different periods and regions worldwide. The upper section of the kiln is a domed firing chamber, c. 0.8 m high with a diameter of c. 1 m and a capacity of about 310 to 340 l (eleven to twelve cubic feet). The dome includes a kiln door that gives access to the firing chamber and that is used to load the kiln. The exit flue measures 0.35 m in diameter and can also be used to stack vessels in the firing chamber. The

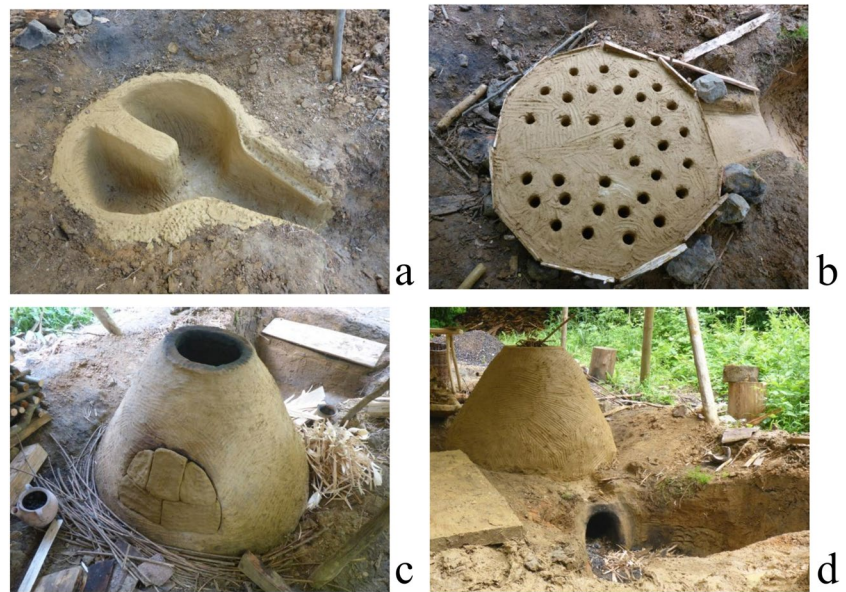
kiln floor is 13 cm thick and is perforated by 34 holes with a diameter of approximately 4 cm each. The combustion chamber is 0.5 m high and 1 m in diameter. The fire channel is approximately 0.5 m long, and its opening has a cross-section of approximately 0.1 m. The structure was built by using a mixture of local calcareous and non-calcareous clays collected in Campus Galli mixed with dung as well as sand collected in a quarry 15 km east of the site.

## Material and methods

### Clay raw materials and their processing

Two different natural clays (Table 1) locally available to Campus Galli were chosen as starting material, a calcareous and non-calcareous one, respectively. This way, we

**Fig. 2** Building phases of the updraft kiln: **a** combustion chamber; **b** kiln floor; **c** firing chamber; **d** fire channel (pictures made by Martin Rogier)



could observe mineralogical and microstructural developments in two types of clay that are known to have a different behaviour during the firing process due to difference of CaO content (Maniatis and Tite 1981). Moreover, the selection of natural clays often characterised by a sandy/silty heterogeneous fraction was preferred over standardised industrial ones, as natural clays are the typical type of materials used in traditional pottery making.

Campus Galli itself is located about 7 km southwest of Sigmaringen, on the edge of the Swabian Jura. The geology of the Swabian Jura consists mostly of Jurassic limestones. Three layers of different limestones are stacked over each other: Black Jurassic, Brown Jurassic, and White Jurassic. Campus Galli is located on the White Jurassic that is marked by different types of limestone formations (the so-called Massenkalk and Hangender Bankkalk) and the occurrence of marls (Fig. 1b). This area is also marked by glacial sediments and erosion layers of the Holocene period. The latter consists of silt with alternating clayey to sandy layers and can have a low calcium content (Bloos et al. 2006).

To make these two clays usable for pottery making, different traditionally known processing techniques particularly suitable for this type of materials (Rice 2015) were applied to produce a calcareous clay paste (A) and a non-calcareous clay paste (F). The calcareous clay was cleaned through a levigation process. The clay was placed for several days in a basin full of water so that the coarser particles in the raw materials were deposited on the bottom, while the suspended fine fraction can be separated. The other clay was cleaned via sieving (mesh size 1.2 mm), but part of the coarser dry fraction was recombined with the finer fraction after soaking in water for several days. In both pastes, approximately 10% quartz-rich sand was added, and the pastes were

homogenised by hand. This sand comes from the same location of the one used to build the kiln structure but was sieved (mesh size 1.2 mm) prior to its usage.

Experimental briquettes were produced by, respectively, mixing pastes A and F with deionised water. The briquettes were dried in controlled conditions at 80° C for 8 h. A series was meant to be fired in the field experiment under actualistic conditions. The other series was meant to be fired in normal air under oxidising conditions in a laboratory kiln (Nabertherm P300) according to a similar temperature profile followed in the kiln experiment in Campus Galli (Supplementary materials).

### Characterisation of the raw materials

To obtain a detailed petrological, mineralogical, and chemical characterisation of the raw material from Campus Galli, samples of pastes A and F were analysed by means of ceramic petrography (Quinn 2013; Whitbread 1995), X-ray powder diffraction (XRPD) (Berthold and Mentzer 2017; Quinn and Benzonelli 2018), Fourier transform infrared spectroscopy (FTIR) (Margenot et al. 2017), and portable X-ray fluorescence (pXRF) (Helfert et al. 2011). Ceramic petrography was performed on thin sections produced from briquettes made from paste A and F and fired in the laboratory at 600 °C, as at this temperature only a minimal thermal alteration of the mineral inclusions present in our pastes would be expected.

XRPD was run on the powdered bulk samples and on their respective clay fraction (< 2 µm). The powders were prepared by grinding into a fine powder unfired samples from paste A and F in an agate mortar, while the pure clay fraction (< 2 µm) was extracted by sedimentation in an



Atterberg column. The concentrated clay fraction suspension was then poured onto two glass slides to produce even and textured samples. This is a well-established method for clay mineral analysis using XRPD in natural sciences (Moore and Reynolds 1997). This way, the 001-intensities from this type of minerals are significantly enhanced, which is a key feature for clay mineral characterisation using XRPD. After drying, both slides were measured to characterise them at room temperature under natural humidity. In a second step, to have a better characterisation of swellable clay minerals such as montmorillonite, one of the slides was saturated at room temperature with ethylene glycol within an exicator for several days and measured again.

By this procedure, the large ethylene glycol molecules are incorporated in the interlayer of swellable clay minerals, resulting in an increase of the c-lattice distance which leads to a decrease in  $2\theta$  angle of the corresponding 001-intensities in the diffractograms.

The instrument used for XRPD analysis was a Bruker D8 advance equipped with a Cu-sealed tube (40 kV/20 mA), a Göbel mirror optics, a 0.2-mm divergence slit, a fixed knife edge to suppress air scatter, and a VÁNTEC 1-detector. The crystalline phases were identified using the PDF data from the 2006 International Centre for Diffraction Data-Joint Committee of Powder Diffraction Standards (ICDD-JCPDS). The powdered bulk samples were rotated during the measurement.

FTIR spectroscopy was also used to identify mineral composition and alteration due to heating. Spectra were collected in transmission using the KBr method between 4000 and 400  $\text{cm}^{-1}$ , at 4  $\text{cm}^{-1}$  resolution with 32 co-added scans using a VERTEX 80v (Bruker) and a Cary 660 (Agilent Technologies) spectrometers. Spectra identification was carried out by using Van der Marel and Beutelspacher (1976) as reference as well as the Kimmel Center for Archaeological Sciences at the Weizmann Institute of Science library of infrared spectra of archaeological materials (Weiner 2010). PXRF was performed by using a Niton XL3t with an experimental method for an external calibration specifically adjusted for the study of ceramics, developed at the University of Frankfurt (Helfert et al. 2011). The advantage of this method is that it is non-destructive, fast, and cost-efficient. However, only a small spot on the sample is analysed, which may not be representative of the composition of the whole specimen. This can be especially problematic for samples lacking a homogenous matrix. In order to minimise potential inaccuracies, three different points in the cross-section of each fragment were measured, and their average was calculated. The results of the pXRF analysis for major and minor elements were normalised to 100% in their oxide form calculated by stoichiometry.

## Characterisation of fired samples

All fired samples (Table 1) were analysed with ceramic petrography to assess their petrographic and mineralogical composition as well as the optical activity of the matrix, as this could give an indication on the firing conditions and temperatures (Quinn 2013, pp. 23–33).

XRPD and FTIR were utilised to provide a detailed mineralogical characterisation of pottery fragments to aid in the reconstruction of their original firing temperature (“archaeothermometry”, see Rice (2015, pp. 99–116)). This method makes use of the presence and absence of mineral phases that are modified, formed, or can disappear at specific temperatures and under specific atmospheric conditions (Berna et al. 2007; Gliozzo 2020; Maggetti 1982; Maniatis et al. 2002; Maritan et al. 2006; Nodari et al. 2007; Shoval and Beck 2005). XRPD and FTIR were run with the same instruments and parameters as above; the XRPD samples were rotated during the measurements.

Scanning electron microscopy (SEM) analysis was used to assess the degree of vitrification, which is a crucial and easily measurable point in pyrotechnological studies (Maniatis and Tite 1975, 1981; Montesana et al. 2019; Tite and Maniatis 1975a, b). A fresh fracture of the samples was platinum-coated, and secondary electron images were taken from the core as well as the margins of the samples via a Hitachi TM3030 + tabletop SEM microscope using an accelerating voltage of (15 kV), an operating current of 110  $\mu\text{A}$ , and a variable working distance at 1000 $\times$  and 2000 $\times$  magnifications.

## Field experiment

### Firing structure

The kiln was not built specifically for this experiment, it had been used already in several firings and represents a very common type of design. Therefore, to monitor the heat impact on the structure caused by our firing experiment, a separate clay brick was prepared. The block was produced by mixing the same type of non-calcareous clay and sand used to produce paste F. However, as a coarser paste was needed this time, the sand was not sieved prior to usage, and additionally, chaff was added as temper. The ratio of these ingredients in the paste was 4:5:1 respectively. After mixing, the brick was carefully shaped and placed into the kiln door.

### Preparation and position of the kiln load

One hundred and thirty-five pots marked by different types of paste were prepared by Martin Rogier, using the local calcareous and non-calcareous clays. Pot shapes range from

simple ollae to large casseroles which are consistent components found in the archaeological record (Fig. 3b). All pots were numbered at the base (nos. 1–135). However, as only 100 vessels could be arranged in the kiln, the rest were left unfired. Similar forms were scattered in different spots and at different heights with the aim of fitting as many pots as possible. The pots were distributed on roughly 5 levels (Fig. 3a). The lower strata of pots were mainly introduced by the lateral opening of the kiln, while only those belonging to the 2 uppermost levels were introduced from the top (Fig. 3c–d). Finally, the kiln load was covered by placing larger broken and already fired shreds on the top, which served as heat insulators for the structure. After this, the later entrance was sealed with pure clay, and a lid was placed on top of the kiln dome.

### Fuel preparation

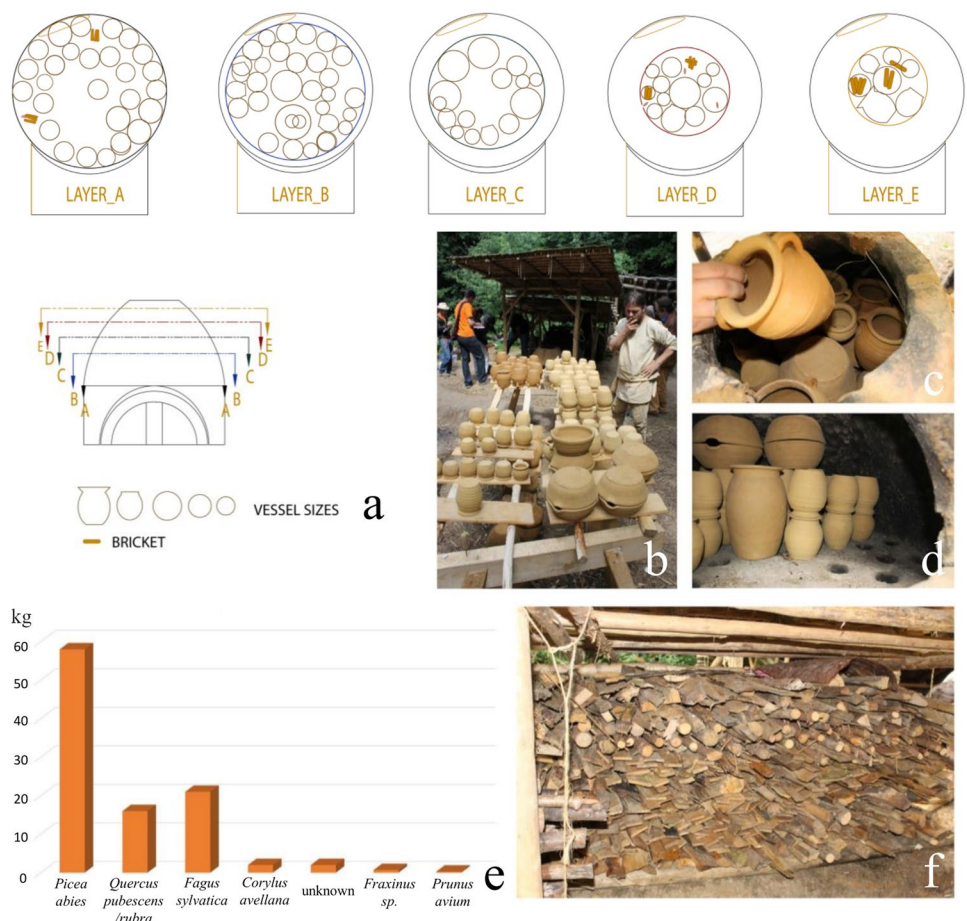
Before the firing process, the fuel was carefully collected and documented (Fig. 3e–f). We decided to use wood as a fuel as this is a well-documented type of material according to several ethnographic studies and was locally available (e.g. Gosselain 1992; Livingstone Smith 2001; Sillar 2007).

The wood assemblage consisted of arboreal taxa found in the proximity of the pottery workshop, i.e. *Picea abies* (spruce), *Quercus pubescens/rubra* (downy and red oak), *Fagus sylvatica* (beech), *Prunus avium* (wild cherry), *Fraxinus* sp. (ash), and *Corylus avellana* (hazel). The largest portion of fuel consumed was from spruce wood (58%), followed by beech (21%). The degree of humidity of the air-dried logs was measured before firing by using a moisture meter that gave an average reading of c. 11 (range c. 9–16), indicative of very dry fuel. The total amount of the fuel, which was measured before the firing, was weighed to a total of 265.15 kg, which mostly consisted of spruce, beech, and oak logs.

### Temperature monitoring

The heat distribution within the kiln and the impact on the kiln structure were monitored using twelve thermocouples attached to three Omega RDXL6SD 6-Channel devices (four for each device). Two thermocouples were positioned in the combustion chamber, and six of them were placed in the upper firing chamber.

**Fig. 3** a Drawing illustrating the position of the vessels within the updraft kiln (Paola Sconzo); b Vessels produced by Martin Rogier; c Stacking of the vessels within the kiln; d Vessels within the kiln; e Graph illustrating the different types of wood used as fuel (Lionello Morandi); f Wood prepared to be used in the firing (pictures made by Silvia Amicone)



The six thermocouples placed in the firing chamber were inserted in the interior of a clay brick of approximately  $2\text{ cm} \times 1\text{ cm} \times 1\text{ cm}$ . This setup was aimed to get a more realistic information of the temperature changes inside a fired ceramic and not only the flame temperature during the whole firing process (Fig. 4). At the same time, a selection of briquettes made from pastes A and F were positioned close to thermocouples 2, 3, and 7 within the firing chamber (Fig. 3a).

Additionally, four thermocouples were placed inside a large brick as a part of the kiln wall 5 cm from one another starting from inside of the kiln wall, so that it was possible to record the heat distribution from the direction of the heat source towards the outer part of the kiln (Fig. 4d). The temperature was measured and recorded automatically every 0.5 s.

### Firing process

The firing procedure started at 06:10 when the fuel was ignited (Fig. 5a) and the opening of the dome was closed, leaving only an aperture of about 16 cm.

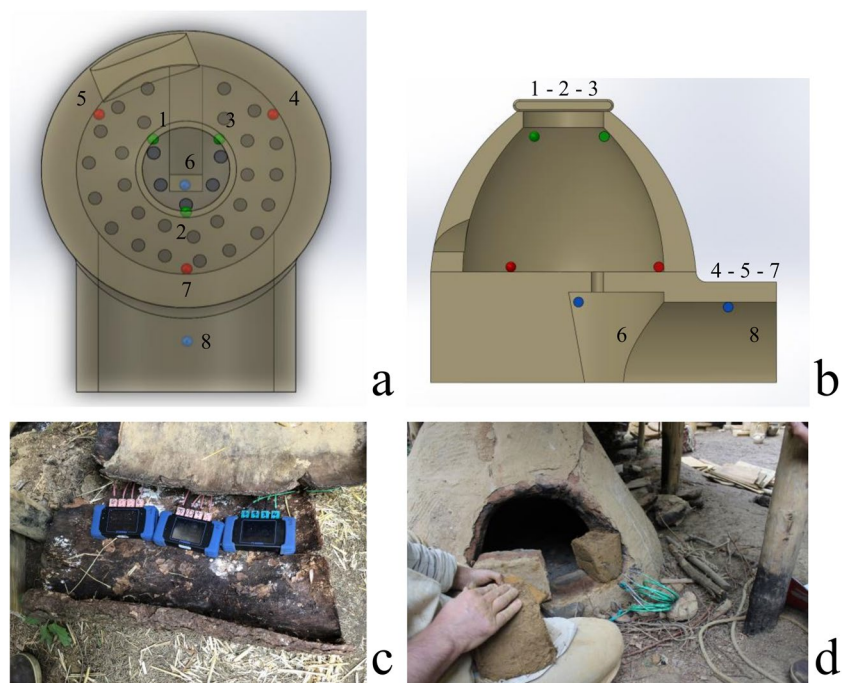
The participants of the experiment were divided into teams to carry out several activities related to the daily routine of a pottery workshop. Such duties included producing additional firewood, kiln maintenance, and the filling of the fuel into the kiln. Two hours after the beginning of the experiment, cracks started to appear on various parts of the kiln structure. These cracks were repaired on the spot by the participants with an ash, water, and cob mixture, a procedure

that continued as part of the kiln maintenance throughout the whole experiment. At 12:55, the upper lid was shortly removed, and thus, black smoke was released. At this stage, the pots, as it could be observed through the top opening, began to become blackish (Fig. 5b). At 14:30, a spyhole in the loading door area was opened to observe the firing of the vessels (Fig. 5c).

Such observations through spyholes helped assess how much more fuel should be added, and what temperature had been reached based on changes in the pots' colour. In the following 2 h, multiple observations were made by opening and closing the spyhole. At 15:50, the lid was removed again, but this time, the smoke was more transparent rather than black. At 17:13, after 11 h of firing, the temperatures indicated by the thermocouples were observed to not be increasing anymore, and the heating rate became extremely slow. The lid, together with the upper layer of broken shreds, was then removed with the help of pliers.

After this, the already burning wood in the firing channel was pushed into the combustion chamber, and the ash that was excessively building up in the channel was removed to the edges of the firing tunnel. The temperatures started rising, and at 19:35, the first flames rose out of the lid (Fig. 5d–e). At 22:43, the last cracks around the kiln were repaired, and the kiln lid was placed on the top again and completely sealed with a wet clay mixture. A slab was also placed to seal the fuel area. Once the kiln was completely closed, the kiln structure was left to cool down overnight, with the temperatures still being recorded.

**Fig. 4** Position of the thermocouples used to record the firing temperature: **a–b** Position of the thermocouples in the firing and combustion chambers (Tobias Kiemle); **c** Omega RDXL6SD devices used to record the firing temperatures; **d** Kiln block with thermocouples (pictures made by Silvia Amicone)





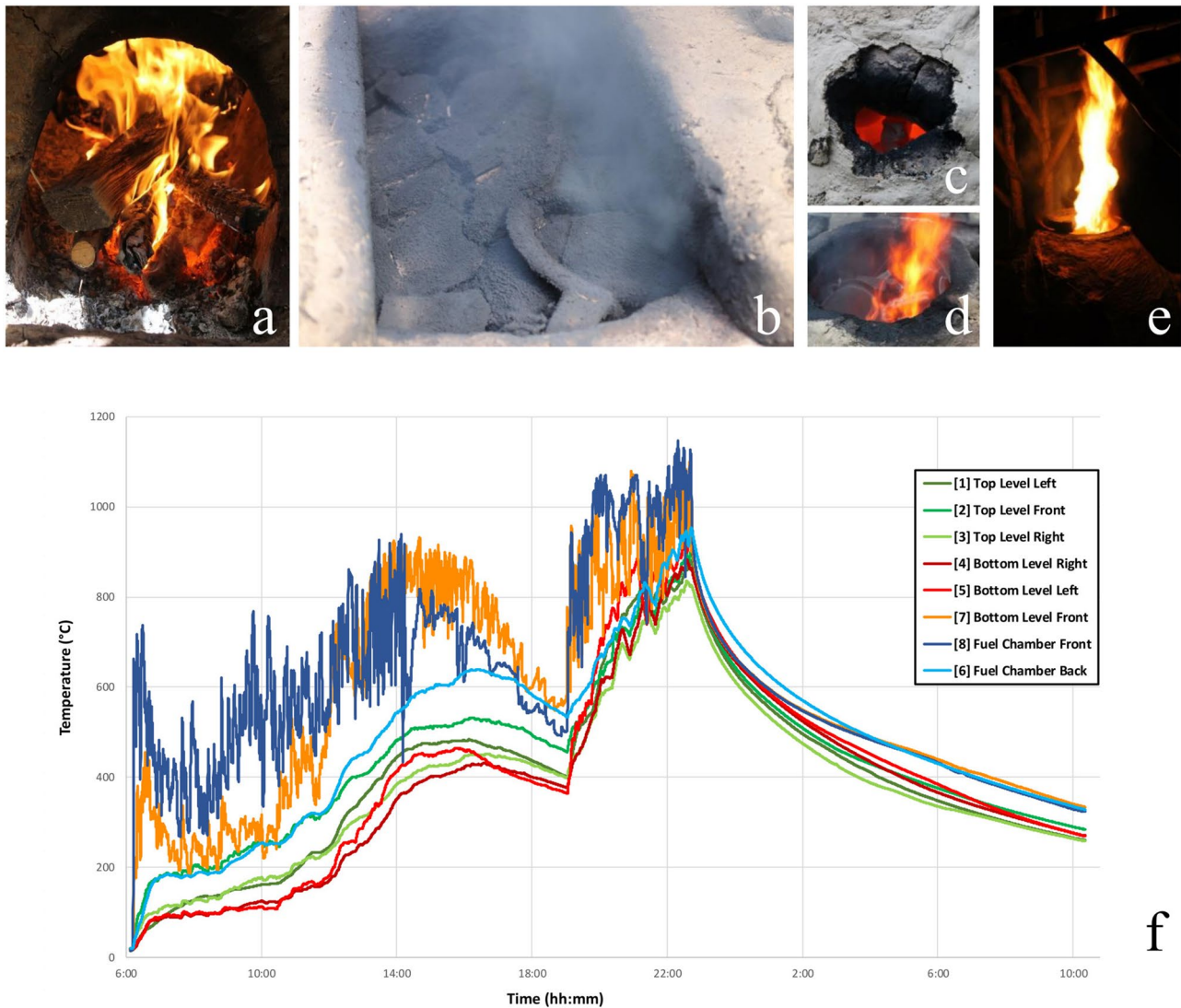


**Fig. 5** a–e Drawings illustrating different moments of the firing (pictures made by Silvia Amicone); f Graph illustrating the temperatures of the thermocouples placed within the kiln (Tobias Kiemle)

## General observations

By looking at the data, it can be observed that the maximum peak temperature around 1150 °C was recorded by the sensor TC8 located at the front of the fuel chamber (Fig. 5f). In the firing chamber, the maximum peak temperature of around 1100 °C was recorded by TC7 located just above the perforated floor (Fig. 5f). The lowest temperature, 835 °C, was recorded by TC1 in the upper part of the firing chamber (Fig. 5f). It is interesting to notice that the maximum temperatures reached by the different thermocouples were recorded only for a few minutes, and then the temperatures directly began to decrease.

The difficulties that we encountered in reaching these temperatures could be explained in different ways such as the kiln design, distribution of the vessels' loading, and type

of fuel as well as weather conditions. However, we cannot exclude that this was due also to imperfect coordination in the addition of fuel, as we realised quite late that there was too much carbon in the firing chamber at a certain point, meaning that too much fuel was added, which could not be properly combusted. At the end of the experiment, 183.65 kg of wood was used. All the pottery fired survived, but some of the vessels showed cracks or black areas due to the difficulties to control the atmosphere during the firing that resulted in more reducing conditions than we had aimed for.

More precisely, cracks at the base occurred on 14 vessels, 14% of the total number. These were generally located in the lowermost level (layer A) and were in direct contact with the kiln floor. The cracking of rims occurred instead mainly on those pieces set in the second layer (layer B). The vessels set in layers C-E were those which instead featured

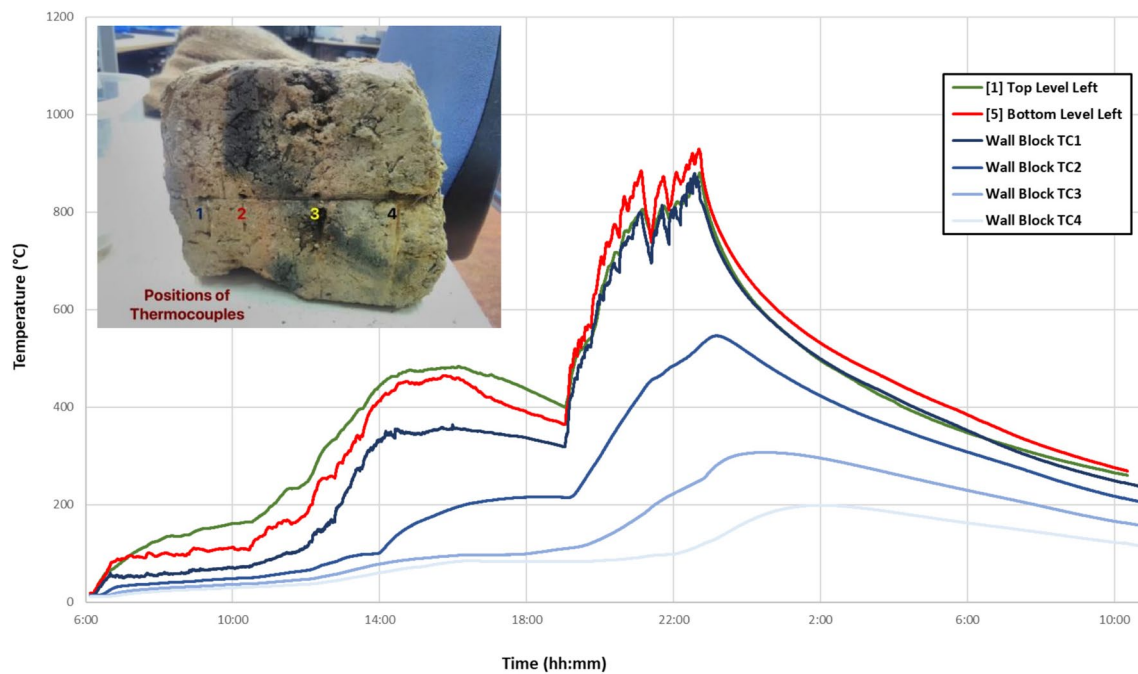


**Fig. 6** Graph illustrating changes in the temperatures of the thermocouples placed within the kiln wall during different phases of the firing (Tobias Kiemle)

blackened patches on the body and on the outside of the rim. Finally, the temperatures recorded in the kiln wall (Fig. 6) were drastically lower than inside the kiln and ranged from 124 to 542 °C in the area untouched by the flames, reaching 878 °C only on the side that was directly in contact with the firing chamber. The kiln structure itself survived the firing rather well, and it is still in use today, but several cracks formed during the process, which constantly required repair.

## Results of the laboratory investigations

### Analysis of raw materials

The results of ceramic petrographic analysis indicate that paste A is medium coarse and relatively poorly sorted (maximum 1 mm, minimum 0.01 mm, average 0.3 mm). It is characterised by the presence of quartz (mono- and polycrystalline), calcite (micritic, less frequently sparitic), feldspars (plagioclase and perthite rarely microcline), chert, opaques, and very rarely glauconite, epidote, and foliated metamorphic rocks composed of quartz, muscovite, and biotite (Fig. 7a–b).

Calcite can occur as very small inclusions (0.01 mm) as well as coarser ones (0.8 mm). The same assemblage of minerals was identified by XRPD analysis (Fig. 7c), but in addition, kaolinite and illite could be identified, with their main peaks at Kln001 ( $d=7.1 \text{ \AA}$ ) and Ill001 ( $d=10 \text{ \AA}$ ) respectively. The

XRD analysis of the clay fraction  $<2 \mu\text{m}$  also reveals the presence of smectite and mixed layer clay minerals (Fig. 7d), which were overseen in the XRPD due to their weak intensities.

Similarly, paste F appears to be medium coarse (maximum 0.8 mm, minimum 0.01 mm, average 0.3 mm) and poorly sorted. It includes quartz (mono- and polycrystalline), calcite (micritic less frequently sparitic, overall, less than in paste A), feldspars (plagioclase and perthite), chert, opaques, and very rarely glauconite and foliated metamorphic rocks composed of quartz, muscovite, and biotite (Fig. 8a–b).

This is confirmed by the results of XRPD analysis (Fig. 8c) that also revealed the presence of chlorite, kaolinite, and illite with their main peaks, respectively at Chl001 ( $d=14.1 \text{ \AA}$ ), Kln001 ( $d=7.1 \text{ \AA}$ ), and Ill002 ( $d=10 \text{ \AA}$ ). Moreover, for paste F, the XRD analysis of the clay fraction indicates the presence of smectite and clay minerals with mixed layers (Fig. 8d).

The FTIR spectra (Figs. 7e and 8e) confirmed that both pastes A and F are dominated by kaolinite as shown by the absorbance bands at 3697, 3621, 1034, 1010, 914, 754, and 538  $\text{cm}^{-1}$  wavenumbers. The presence of quartz in both pastes is also evidenced by the shoulder around 1085  $\text{cm}^{-1}$  wavenumbers and the doublet at 798 and 779  $\text{cm}^{-1}$  wavenumbers. The main difference between pastes A and F is the higher amount of calcite in paste A, which is indicated by the absorbance bands at 1431, 875, and 712  $\text{cm}^{-1}$  wavenumbers. In paste F, the presence of calcite is marked only by a weak absorbance band at 1431  $\text{cm}^{-1}$  wavenumbers.

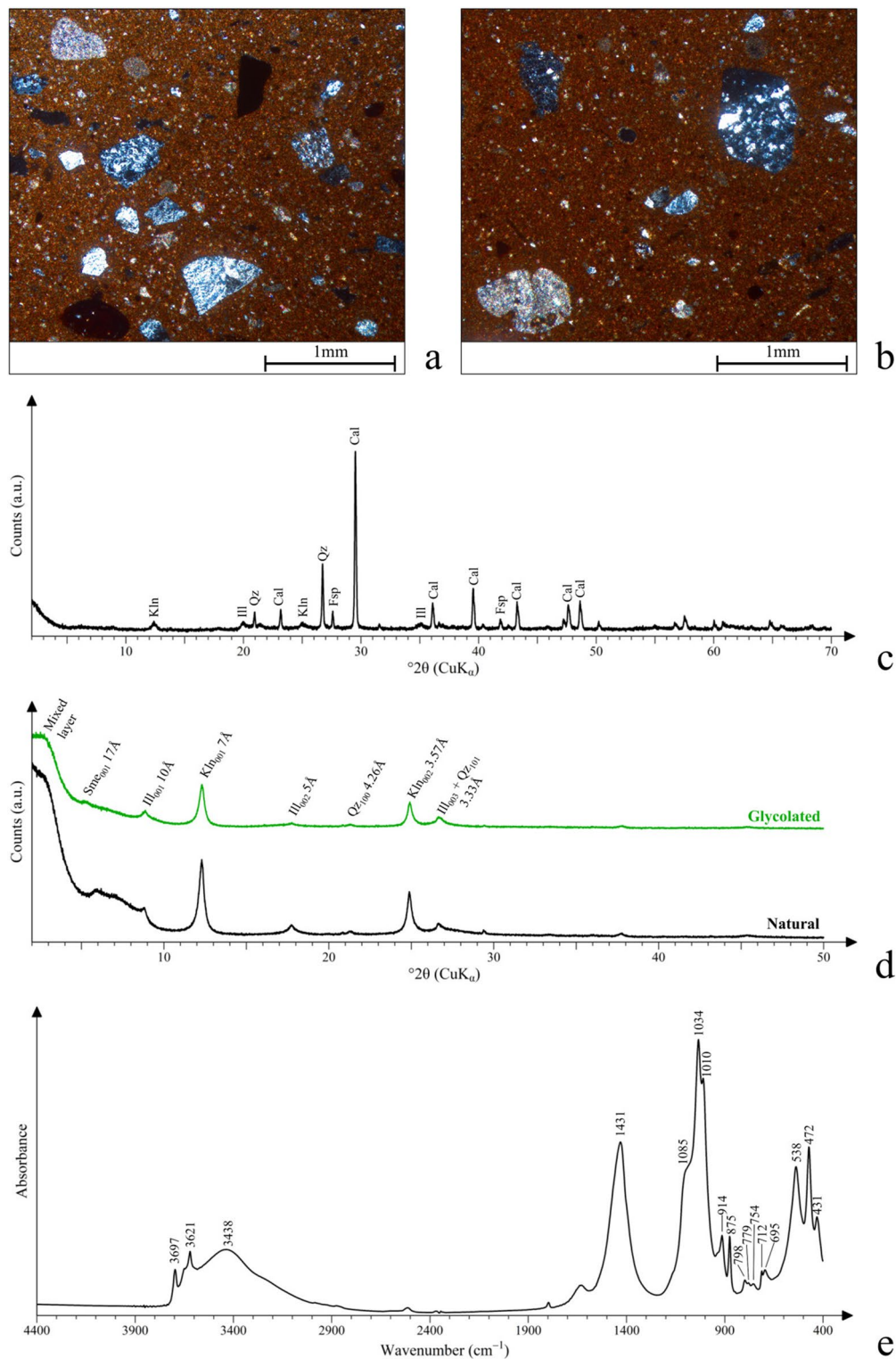


**Fig. 7** Results of laboratory analyses carried out on paste A before firing: **a–b** results of petrographic analysis; **c–d** results of XRD analysis; **e** results of FTIR analysis

The pXRF analysis (Table 2) showed that the two pastes have considerable compositional differences. Paste F has a very low concentration of CaO (c. 2 wt %), while paste A contains c. 35

wt % of CaO. On the other hand, the concentration of SiO<sub>2</sub> and Fe<sub>2</sub>O<sub>3</sub> is higher in paste F (c. 66 wt % and c. 7 wt %, respectively) relative to paste A (c. 39 wt % and c. 5 wt %, respectively).

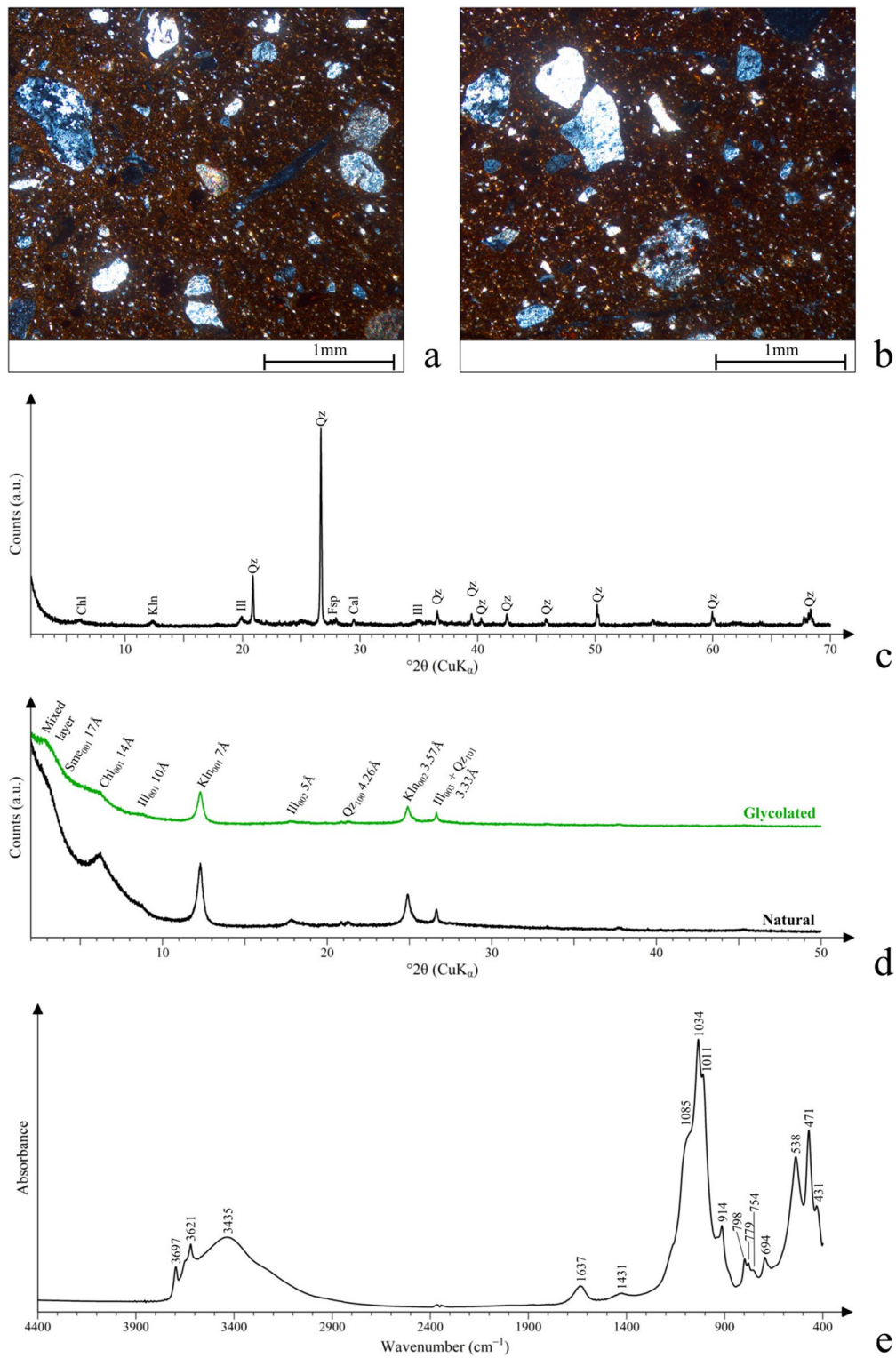


**Fig. 8** Results of laboratory analyses carried out on paste F before firing: **a–b** results of petrographic analysis; **c–d** results of XRD analysis; **e** results of FTIR analysis

**Table 2** Results of the pXRF results (expressed as wt %), showing the normalised major and minor elements

Sample	SiO <sub>2</sub>	TiO <sub>1</sub>	Al <sub>2</sub> O <sub>3</sub>	Fe <sub>2</sub> O <sub>3</sub>	MnO	MgO	CaO	K <sub>2</sub> O	P <sub>2</sub> O <sub>5</sub>	TOTAL
Paste A	38.87	0.63	17.70	4.57	0.06	1.02	35.28	1.77	0.11	93.25
Paste F	66.24	1.45	19.73	7.19	0.14	1.76	1.69	1.59	0.23	98.27

## Analysis of experimental samples

### Paste A

The XRPD results (Fig. 9a) show that in both samples (field and lab experiments) made from paste A and fired at 835 °C, kaolinite and illite reflections disappeared completely from the diffractograms, while feldspars and calcite reflections decreased their intensity. However, the main peak of calcite ( $2\theta=29.41^\circ$ ) appears to be weaker in the sample fired in the laboratory. Finally, a mineral of the melilite group with gehlenite composition shows up as a new phase and is visible from the appearance of its main reflection at  $2\theta=31.42^\circ$ . The slight shift of the main intensity could indicate a certain Mg content.

The FTIR results (Fig. 9b) also show that calcite is thermally altered, suggesting an incipient formation stage of aragonite. This is indicated by the broadening of the main calcite absorbance band, which started to form a shoulder at  $1446\text{ cm}^{-1}$  wavenumbers and by the formation of absorbance band at  $858\text{ cm}^{-1}$  wavenumbers (Toffolo and Boaretto 2014). The main peak of the kaolinite at  $1034\text{ cm}^{-1}$  is no longer visible and is replaced by a broad band with peaks at  $1017, 977, 919,$  and  $800\text{ cm}^{-1}$  wavenumbers, which best fit with sorosilicate minerals of the melilite group. The paste that was heated in the laboratory oven exhibits a more pronounced aragonite presence, while the absorbance band of the silicate minerals is represented by a broad band with one peak at  $1001\text{ cm}^{-1}$ , which probably points to a more amorphous state.

In thin section, glauconite changed its interference colour from green to reddish due to the oxidation of iron. In addition, some of the muscovite inclusions present in the samples lost their typical interference colour and biotite tended to become reddish-brownish due to oxidation. Calcite is still clearly detectable, but only few grains of sparitic calcite still show the pastel interference colours typical of this mineral, while most calcite inclusions look brown (Fig. 9c, f). The matrix is mostly isotropic in both samples. Under the SEM, the formation of a glass phase can be recognised from the smooth appearance of the matrix, and fine bloating pores can also be observed in the sample fired in the laboratory (Fig. 9i, l).

At 900 °C, the calcite intensities became weaker in the sample fired in the kiln experiment, but they are no more visible in the specimen fired in the laboratory. Feldspar reflections became weaker too, whereas gehlenite reflections became stronger (Fig. 9a). FTIR spectra of the experimental kiln and of the laboratory firing show a similar picture of a somewhat more pronounced aragonite

formation and the presence of a silicate mineral fitting with the melilite group (Fig. 9b).

Under the polarising microscope, only a few grains of sparitic calcite still show interference colours, but this is limited to the samples fired in the field. In both types of samples, small micritic calcite inclusions now look very darkish brown, while larger grains are dark brown and light-yellowish brown in places (Fig. 9d, g), and the matrix shows a completely isotropic behaviour. The SEM images indicate the formation of bloating pores that are sometimes up to  $20\text{ }\mu\text{m}$  in size (Fig. 9j, m).

At 1100 °C, very weak calcite and feldspar reflections are visible in both samples (Fig. 9a). Wollastonite appears as a new phase with a main reflection at  $2\theta=29.98^\circ$ .

The FTIR analysis of both samples shows again the presence of sorosilicate minerals of the melilite group (Fig. 9b). It is interesting to note that in the sample fired in the laboratory, the peaks related to the carbonates are stronger than in the sample fired in the kiln. In the first spectrum, the main absorbance band of calcite is also broader due to being composed of several peaks that are related to heated calcite, aragonite, and other polymorphs of calcium carbonate. On the other hand, the carbonate minerals in the spectrum from the field experiment show a relatively low and broad absorbance band with two clear peaks, one of calcite ( $1420\text{ cm}^{-1}$  wavenumbers), and the other one of aragonite ( $1476$  as well as a weak peak at  $857\text{ cm}^{-1}$  wavenumbers).

In the thin sections of the sample fired in the experiment, the calcite grains no longer show any interference colours and appear completely brown in colour, while in the specimen fired in the laboratory, these are no longer detectable. Feldspar inclusions also look thermally altered, especially in the sample fired in the laboratory. The matrix behaves perfectly isotropic (Fig. 9e, h). Under the SEM, the pores were significantly reduced in size, and the structure appears denser and less porous (Fig. 9k, n).

### Paste F

In the samples made from paste F fired at 835 °C, XRPD results show that nothing changed in the phases' assemblage of the sample fired in the field, while the main calcite peak disappeared in the specimen fired in the laboratory (Fig. 10a). The FTIR spectra (Fig. 10b) of both samples show similar changes in the clay structure, such as the disappearance of the absorption bands at  $3697$  and  $3621\text{ cm}^{-1}$  (loss of structural water), as well as the Al–O–H absorption



band at  $914\text{ cm}^{-1}$  and the Si–O–Al band at  $538\text{ cm}^{-1}$ . Another shift of the main Si–O–Si silicate absorption band occurs from  $1034$  to  $1084\text{ cm}^{-1}$  and a broadening of this band, which is typical for kaolinite heated to temperatures as high as  $800\text{--}900\text{ }^{\circ}\text{C}$  (Friesem et al. 2014). The FTIR resolution is not sensitive enough to detect any calcite left in the clay, but the doublet of the quartz becomes more prominent.

In thin section (Fig. 10c, f), glauconite, muscovite, and biotite changed their interference colour similar to observations in the samples made from paste A. Calcite grains are still clearly visible, but they are thermally altered, and in most cases, they appear brown, occasionally showing reaction rims. The matrix still shows a low optical activity, but only in the specimen from the field experiment. Vitrification was not observed under the SEM in both samples (Fig. 10i, l).

At  $900\text{ }^{\circ}\text{C}$ , the calcite and illite intensities are hardly visible in the diffractogram. The remaining phases are unchanged (Fig. 10a) but in the sample fired in the laboratory at  $900\text{ }^{\circ}\text{C}$  weak haematite reflections can be detected at  $2\theta$  angles of about  $33.2^{\circ}$  and  $35.7^{\circ}$ . The main change of the FTIR spectra (Fig. 10b) is the further shift of the main silicate absorption band from  $1084$  to  $1085\text{ cm}^{-1}$  and broadening of this band. Under the polarising microscope, no calcite grains show typical interference colours, varying from light brown to dark brown. Some grains still display reaction rims (Fig. 10d, g). The matrix has an isotropic behaviour, and both samples exhibit an initial degree of vitrification under SEM (Fig. 10j, m).

Newly formed phases could not be identified via XRPD at  $1100\text{ }^{\circ}\text{C}$ , but, in the sample fired in the laboratory, haematite intensities increased, while the feldspar reflections decreased considerably (Fig. 10a). No additional changes were visible in the FTIR (Fig. 10b). In thin section, few calcite inclusions are still visible, but they appear completely dark brownish, while feldspars show characteristics of thermal alteration, especially in laboratory samples (Fig. 10e, h). The feldspars sometimes appear thermally altered, while the matrix is completely isotropic. The structure of the ceramic under SEM shows extensive signs of vitrification (Fig. 10k, n).

### Analysis of the kiln block

Quartz, feldspars, calcite, and illite could be detected in all four samples taken from the block (Fig. 11a). Additionally, weak diffraction peaks of chlorite and amphibole are observable in all the samples apart from TC1, respectively, at about  $2\theta = 12.6^{\circ}$  and  $2\theta = 10.4^{\circ}$ . Similarly, kaolinite and dolomite were detected in all the samples apart from TC1, respectively, at around  $2\theta = 12.3^{\circ}$ , and  $2\theta = 30.9^{\circ}$ .

FTIR spectra showed changes at different temperature ranges (Fig. 11b). The spectra of TC4 and TC3, with temperatures of  $124.7\text{ }^{\circ}\text{C}$  and  $268.1\text{ }^{\circ}\text{C}$ , indicate the presence

of kaolinite, calcite, quartz, and some organic matter and showed no significant shift in any absorption bands. This suggested that no significant structural transformation occurred at these temperatures. The spectrum of sample TC2, which was exposed to temperature of  $542.3\text{ }^{\circ}\text{C}$ , exhibits several changes compared to TC3 and TC4. The spectra of TC2 and TC1, which were exposed to temperatures of  $542.3\text{ }^{\circ}\text{C}$  and  $878.4\text{ }^{\circ}\text{C}$ , respectively, exhibit the common changes of heated clay spectra such as the disappearance of the absorbance bands at  $3698$ ,  $3621$ ,  $915$ , and  $536\text{ cm}^{-1}$  and the broadening and shift of the main silicate band to higher wavenumbers (Berna et al. 2007; Forget et al. 2015).

Under the polarising microscope (Fig. 11c–j), the major changes observed regard the organic and inclusions. In samples TC4 and TC3, exposed to  $124.7\text{ }^{\circ}\text{C}$  and  $268.1\text{ }^{\circ}\text{C}$ , respectively, (Fig. 11c, f), calcite is basically unaltered, and organic materials started to burn; the vegetal fibres, however, are still detectable. In sample TC2 (Fig. 11g, h), exposed to  $542.3\text{ }^{\circ}\text{C}$ , calcite is well detectable and still recognisable from its distinctive interference colour, while the combustion of organic components left voids often filled with charred materials. In sample TC 1 (Fig. 11i, j), exposed to  $878.4\text{ }^{\circ}\text{C}$ , calcite started to decompose. Most of the inclusions show a brown colour and display reaction borders. The organic material is fully combusted.

## Discussion

### Minerals' heat alteration

Some observations can be made on the different mineralogical developments within the samples fired in the kiln experiment under uncontrolled and variable atmospheric conditions, as well as on the specimens fired in the laboratory under controlled oxidising conditions. The behaviour of calcite is particularly worthy of interest. This mineral is still detectable in our samples beyond the expected temperature of its conversion to calcium oxide, occurring between  $675$  and  $800\text{ }^{\circ}\text{C}$  (Gliozzo 2020). Certainly, it is not possible to exclude that some of this calcite could be secondary, as this latter forms through the carbonation of calcium oxide. This is suggested, for example, by the broadening of the main calcite reflection ( $2\theta = 29.41^{\circ}$ ) observed in both XRPD diffractograms of the fired samples made from pastes A and F exposed to the fire (Fig. 9a). With FTIR, an attempt to identify secondary calcite in the spectra by calculating the calcite  $\nu$  ratio (Chu et al. 2008; Regev et al. 2010) was not successful due to the presence of the absorption bands of the sorosilicate minerals.

On the other hand, secondary calcite can also be recognised under a polarising microscope from the appearance in the fired samples of micritic calcite with moderate

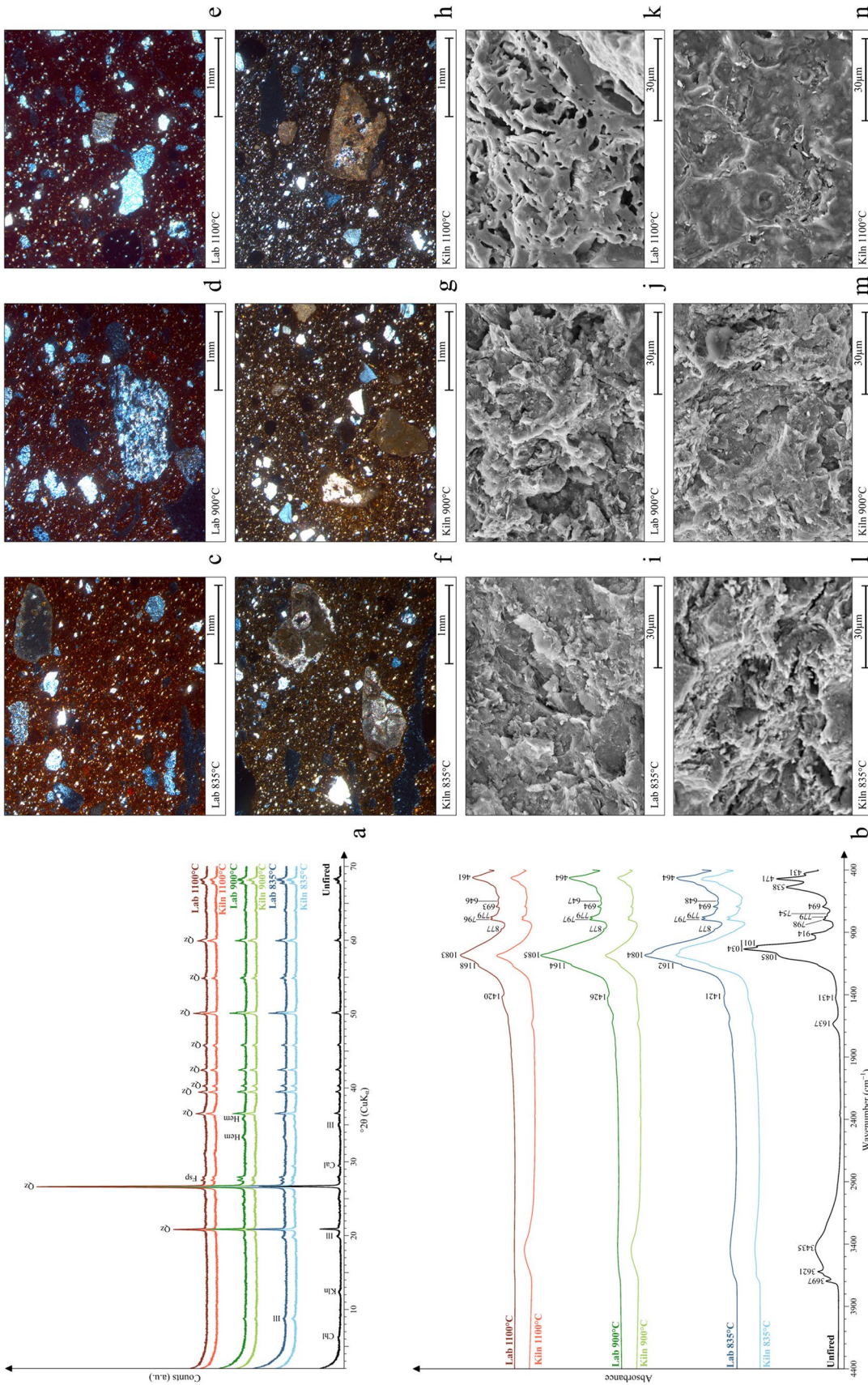


**Fig. 10** Results of laboratory analysis carried out on samples made from paste F after firing in the updraft kiln experiment and in the laboratory: **a** results of XRD analysis; **b** results of FTIR analysis; **c-h** results of petrographic analysis; **i-n** results of SEM analysis



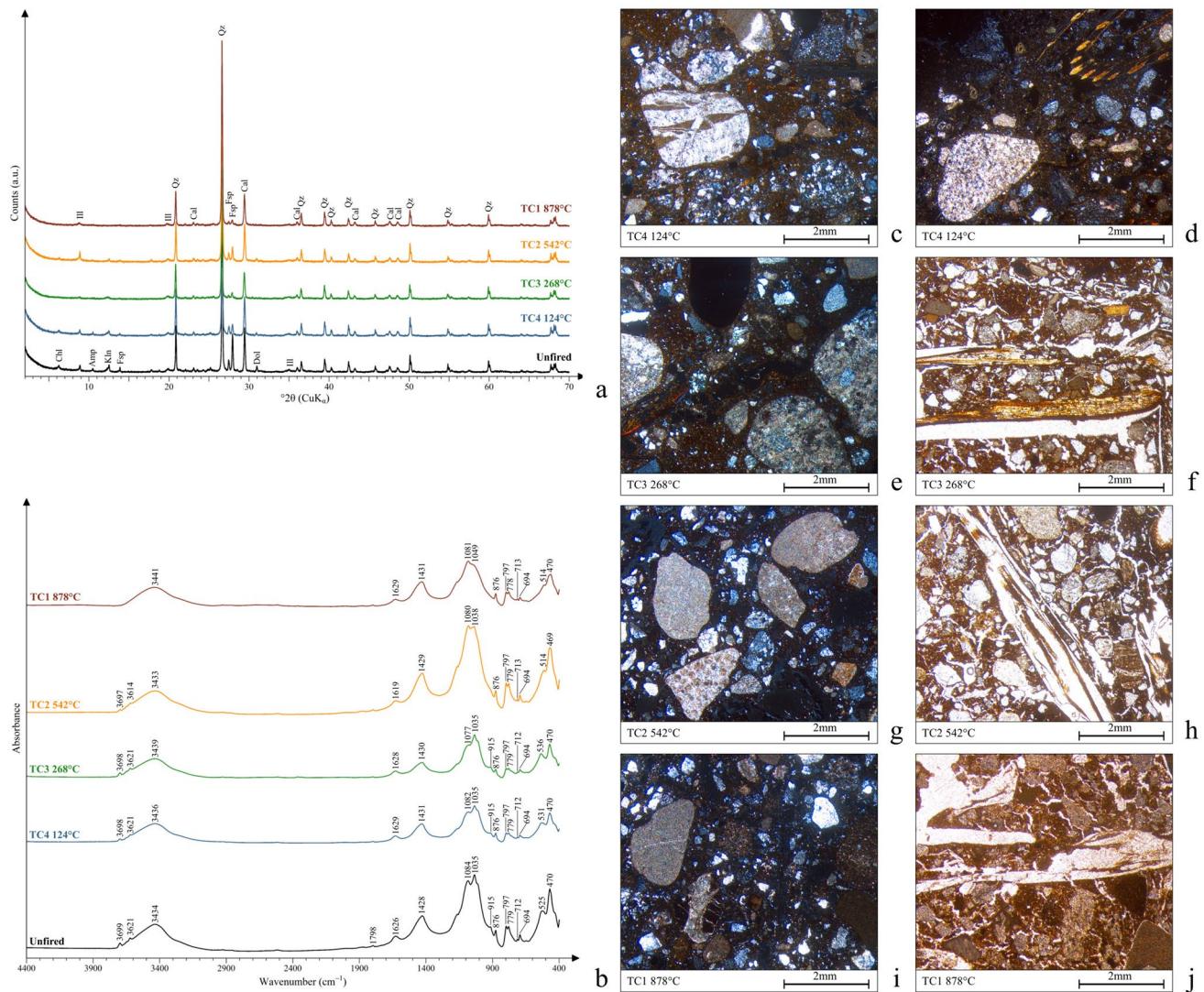


**Fig. 11** Results of laboratory analyses carried out on the kiln block: **a** results of XRD analysis; **b** results of FTIR analysis; **c–j** results of petrographic analysis

low-order bronze/brown birefringence colours (Karkanas 2007). Nevertheless, some of the larger sparite calcite inclusions still show typical primary calcite high-order pastel interference colours at temperatures as high as 900 °C. However, it is known that calcite can resist for longer times at elevated temperatures in coarse and well-crystalline form (Fabbri et al. 2014). Another factor that may have played a role lies in the kinetics of the calcite decomposition, in other words the short soaking time to which all our samples were exposed to (Heimann and Maggetti 2019). In addition, for the very calcareous paste A, the possible excess amount of calcite with respect to the availability of silicates may have caused an incomplete reaction between CaO and the relict of the clay minerals (Fabbri et al. 2014). Within the calcareous samples, this delay in the decomposition of calcite is particularly

pronounced in the specimens fired in the kiln in Campus Galli. For example, looking at the microstructure of the two sets of samples made from the calcareous paste A, it is evident that the formation of bloating pores resulting from the decomposition of calcite appears only at 900 °C and only in the sample fired in the field. This is likely due to the atmospheric conditions during our field experiment, which were variable and definitively more reducing compared to those in the laboratory firing experiment, as mentioned above. It is known that for the same clay fired under reducing conditions, the stability of calcite is increased by 100 °C (Heimann and Maggetti 2019; Maniatis and Tite 1981). In general, in the case of field experiments, the large temperature gradient within the kiln and the sample itself, the heterogeneity of the paste, and the related uneven distributed reaction partners play

a role in affecting the delayed decomposition of calcite (Fabbri et al. 2014). On the other hand, it is interesting to note that clay minerals such as illite and kaolinite cannot be found, as expected, beyond the temperature threshold (Gliozzo 2020) at which they are supposed to decompose (c. 900 °C) or transform into metakaolinite, respectively (c. 650–700 °C). In addition, gehlenite that normally forms from the reaction of CaO and the decomposition of clay minerals at about 800 °C in oxidising and 850 °C in reducing conditions, respectively, is found at the usual temperatures in samples made from paste A (Heimann and Maggetti 2019). This means that despite the delay in the complete transformation of calcite into calcium oxide, there is still enough Ca to react with the relict of the clay minerals to form gehlenite. Clearly, we also have to bear in mind that other Ca-containing fine-grained minerals beside calcite, such as smectites, could provide a certain amount of Ca content.

Finally, some interesting remarks can be included for samples made from paste F. In none of these specimens, gehlenite could be detected due to the low concentration of calcite within this paste. However, because of the higher iron concentration that marks this paste, haematite could nucleate in the samples fired in the laboratory. This mineral usually forms over a wide range of temperatures from 400/450 to 850 °C, provided that the original clay has an adequate iron content and that is fired under oxidising conditions (Gliozzo 2020). The absence of iron oxides in the samples fired in the kiln, such as magnetite and hercynite, which normally form in the same range of temperatures under reducing conditions, suggests that there was still too much oxygen in the system, preventing the nucleation of these minerals.

Overall, the results clearly show that kinetics, i.e. the dynamic nature of the firing process, imposes constraints on thermodynamics by retarding some reaction rates in all our samples. True thermodynamic equilibrium could not be achieved because of too short reaction times in combination to relatively low, large temperature gradients in the kiln, heterogeneously distributed reaction partners, and varying redox conditions (Heimann and Maggetti 2019) typical for an updraft kiln firing profile.

### Limits and potential of different analytical methods

The application of an integrated archaeometric approach allowed us to further explore the potential and limits of the different techniques applied. Ceramic petrography is clearly a very useful technique to study calcite modifications, as it allows a detailed detection of the progressive alteration of this mineral and its interaction with silicates through the change of its interference colour, the appearance of reaction rims, and the formation of secondary

calcite (Karkanas 2007). Moreover, through thin-section petrography, it is possible to observe the alteration of other minerals which, due to their low concentrations, are not detectable via other methods, such as XRPD or FTIR. In our case, this is well evident for minerals such as glauconite, biotite, and muscovite. This is also true for different types of feldspars, whose precise nature and alteration can be studied in detail only through optical microscopy. In addition, with this technique, we were able to study thermal alteration of organic materials such as plant matter, which is very useful to understand low-temperature modifications. Finally, ceramic petrography also allowed us to acquire some initial understanding of the vitrification from the evaluation of matrix optical activity and related anisotropic or isotropic behaviour. Nevertheless, it is important to bear in mind that optical activity tends to be exaggerated in parts of the slide that are < 30 µm thick, and it is often not as easily visible in dark fired ceramic under reducing conditions (Quinn 2013, p. 94). In this regard, SEM is the best technique, as it allows to assess more precisely the degree of vitrification as well as the formation of bloating pores due to gas release within ceramic during firing (Maniatis and Tite 1981).

When it comes to assessing low-temperature mineral alteration of clay materials, the most effective technique seems to be FTIR. This method allowed us to see clay mineral alteration at relatively low temperatures through the disappearance of the absorbance hydroxyl bands, at 3698 and 3622, 915, and 536 cm<sup>-1</sup>. This was observed for example in the TC2 sample exposed to 542 °C. The same sample analysed with XRPD did not show significant alteration at this temperature. FTIR also allows the detection of secondary calcite by observing the shift of the CO<sub>3</sub> band (Fabbri et al. 2014, p. 1908) and the formation of aragonite that normally starts to nucleate when calcareous minerals are exposed to temperatures higher than 600 °C (Toffolo and Boaretto 2014). In our study, its presence can be suggested by the broadening of the main calcite absorbance band, which starts to form a shoulder at 1446 cm<sup>-1</sup> wavenumbers and the formation of an absorbance band at 858 cm<sup>-1</sup> wavenumbers. Remarkably, it was not possible to detect aragonite via XRPD, probably because the concentration is below the detection limit in the percent range and/or the newly formed pyrogenic aragonite is very poorly crystalline and, therefore, also difficult to identify with this technique (Toffolo and Boaretto 2014).

On the other hand, XRPD helps to study the nature of clay minerals and the neoformation connected to higher temperatures with an incomparable degree of resolution. In this specific case, the use of XRPD allowed the identification of the clay mineral mixture present in our samples and the nucleation of haematite, gehlenite, and wollastonite.

## Archaeological implications

One observation concerns a certain difficulty to control the temperatures and atmospheric conditions in our firing experiment in the updraft kiln. In several studies, the authors tend to claim a direct connection between thermal profiles and the types of installations, and they often contrast “open firings” with “kiln firings” (e.g. Gibson and Woods 1990; Kingery 1997; Rye 1981; Tite 1995). The first type of firing should be relatively short, reach lower temperatures, and be more difficult to control, while kiln firings should have the advantage of reducing the effects of prevailing winds and the time to reach the maximum temperatures. In addition, such installations could facilitate controlling the duration of the soaking time, redox conditions, and slow down the cooling process (Cuomo di Caprio 2007, pp. 508–526).

However, as clearly shown by the systematic experiments run by Thér and colleagues (Thér et al. 2019), each type of installation is characterised by various possible firing procedures, and the advantages of using kilns are at the same time largely influenced by the type of kiln that is utilised. Therefore, firing in a simple kiln where fuel is in direct contact with the vessels could produce a similar firing profile, as well as difficulties regarding the control of several parameters, like those experienced in open firings (Amicone et al. 2021). Moreover, as our experiment clearly showed, the skills of the people involved in the activity have a large impact in the firing procedures. While our firing was supervised by an expert potter, the involvement of large numbers of early practitioners in the process caused at times an inefficient rhythm in the fuel charging that resulted in an irregular thermal profile and variable atmospheric conditions. Overall, the above suggests that archaeologists should take care to ask themselves the right questions when addressing the topic of ceramic pyrotechnology. In the first instance, as discussed above, a direct relationship can only be drawn between pottery characteristics and firing procedures and not necessarily between pottery and the type of firing installations (Amicone et al. 2021; Thér et al. 2019). This is also true in respect to another imperative question in ceramic pyrotechnological studies, i.e. the estimation of maximum firing temperatures. As our experiment and other studies have shown (e.g. Maggetti et al. 2011), the huge gradient that characterised traditional firing implies that vessels fired in the same process or even portions of the same vessel could be exposed to drastically different temperatures. This leads us to the conclusion that, when addressing ancient pyrotechnology, the scholars should focus on reconstructing different aspects of the overall firing profile, rather than only on maximum firing temperatures reached. This knowledge would be more informative of the technological level achieved by the pottery manufacturers and their skills while allowing the investigators to better explore the social

implications of their studies. Finally, our detailed mineralogical study strongly suggests that scholars carrying out analysis on ceramics or ceramic installations to reconstruct pyrotechnological processes should always formulate their interpretation with caution. This situation arises from the fact that mineral assemblages, as well as microstructures identified in ceramic materials (e.g. grain-sized distribution of the reaction partners, homogeneity of the material, mean statistical distribution of all reactants), are often miles away from real thermodynamic rules. This means the thermodynamic equilibrium will not be reached due to kinetic effects (too short reaction times) but also due to this pure “mechanistic” situation of the material properties (Heimann and Maggetti 2019). This implies that, aside from being able to master the execution and interpretation of several analytical methods, scientists should also be aware of the complex dynamics of firing in traditional crafts and should carry out the sampling in the field, together with archaeologists. For example, our experiment showed that when studying firing installation, the position of the sample within the structure is a crucial parameter to make meaningful interpretations on its thermal alteration. As discussed above, this is due to the fact that different areas of these structures may have been exposed to a drastically diverse range of temperatures.

## Conclusions

Through our experiment we were able to document the entire firing process in one of the most common firing installations of the ancient world. This was possible with the helpful participation of a large group of students and scientists involved in the experiment whose joint efforts allowed us to achieve a practical experience of traditional firing in an updraft kiln and its challenges. At the same time, through our integrated interdisciplinary approach, we produced an important dataset that can be expanded upon in future investigations, while providing an important analogue for the interpretation of archaeological kilns from a wide global and temporal range.

Our results further highlight the limits and potential of different analytical tools frequently used to study ceramic pyrotechnology. Most importantly, this experiment provided general guidelines for archaeological scientists on how to address the right research questions, develop correct sampling strategies, and choose the appropriate analytical methods for the investigation of ancient ceramic pyrotechnology.

**Supplementary Information** The online version contains supplementary material available at <https://doi.org/10.1007/s12520-023-01798-1>.

**Acknowledgements** This project was carried out in the frame of the Memorandum of Understanding (Lern- und Forschungsort) between the Competence Center Archaeometry – Baden-Wuerttemberg (University of Tübingen) and Campus Galli (southern Germany). In the frame of

this project, Alisa Memmesheimer and Awais Mohammed Qarni carried out their MSc dissertations in Geosciences and Geoarchaeology, respectively. We gratefully acknowledge the Campus Galli staff and volunteers as well as the students of the University of Tübingen for assistance in the preparation of the experiments. We would like to thank in particular the director Campus Galli Dr. H. Napierala for supporting this event and Dr. Susan M. Mentzer for her advices on the FTIR measurements. We would also like to acknowledge the Excellence Initiative (Eberhard Karls Universität Tübingen) and the Ministry for Science, Research, and Art of Baden-Württemberg, as well as the Helmut Fischer GmbH, Institut für Elektronik und Messtechnik for supporting this research.

#### Author's contribution

Amicone, S. conceptualisation; methodology; supervision, formal analysis; investigation; writing, original draft; review and editing, original and final draft; visualisation; and project administration.

Memmesheimer, A. methodology; formal analysis; investigation; and review and editing, final draft.

Solard, B. methodology; formal analysis; investigation; review and editing, original and final draft; and visualisation.

Gur-Arieh, S. methodology; formal analysis; investigation; and review and editing, original and final draft.

Rogier, M. methodology; investigation; review and editing, final draft; visualisation; and resources.

Qarni, M. A. methodology; formal analysis; investigation; and review and editing, final draft.

Seidler, J. methodology; investigation; and review and editing, final draft.

Sconzo, P. methodology; investigation; review and editing, final draft; and visualisation.

Heinze, L. methodology; investigation; formal analysis; review and editing, original and final draft; and visualisation.

Morandi, L. F. methodology; investigation; review and editing, original and final draft; and visualisation.

Kiemle, T. methodology; investigation; review and editing, final draft; and visualisation.

Miller, C. E. methodology; supervision, formal analysis; investigation; review and editing final draft; and resources.

Nickel, K. G. methodology; supervision, formal analysis; investigation; review and editing final draft, resources.

Berthold, C. methodology, supervision, formal analysis; investigation; review and editing, original and final draft; resources; and funding acquisition.

**Funding** Open Access funding enabled and organized by Projekt DEAL.

**Data availability** The authors confirm that the data supporting the findings of this study are available within the article and its supplementary materials. Videos of the experiment are available under these links: <https://youtu.be/r3O8e6zixrw> and <https://youtu.be/wJ55je5AuAc>.

#### Declarations

**Ethical approval** Not applicable.

**Competing interests** The authors declare no competing interests.

**Open Access** This article is licensed under a Creative Commons Attribution 4.0 International License, which permits use, sharing, adaptation, distribution and reproduction in any medium or format, as long as you give appropriate credit to the original author(s) and the source, provide a link to the Creative Commons licence, and indicate if changes were made. The images or other third party material in this article are included in the article's Creative Commons licence, unless indicated otherwise in a credit line to the material. If material is not included in

the article's Creative Commons licence and your intended use is not permitted by statutory regulation or exceeds the permitted use, you will need to obtain permission directly from the copyright holder. To view a copy of this licence, visit <http://creativecommons.org/licenses/by/4.0/>.

#### References

- Amicone S, Forte V, Solard B, Berthold C, Memmesheimer A, Mirković-Marić N (2021) Playing with fire: exploring ceramic pyrotechnology in Late Neolithic Balkans through an archaeometric and an experimental approach. *J Archaeol Sci Rep* 37:102878. <https://doi.org/10.1016/j.jasrep.2021.102878>
- Berna F, Behar A, Shahack-Gross R, Berg J, Boaretto E, Gilboa A, Sharon I, Shalev S, Shilstein S, Yahalom-Mack N, Zorn JR, Weiner S (2007) Sediments exposed to high temperatures: reconstructing pyrotechnological processes in Late Bronze and Iron Age Strata at Tel Dor (Israel). *J Archaeol Sci* 34(3):358–373. <https://doi.org/10.1016/j.jas.2006.05.011>
- Berthold C, Mentzer SM (2017) X-ray microdiffraction. In: Nicosia C, Stoops G (eds) *Archaeological Soil and Sediment Micromorphology*. John Wiley & Sons, Hoboken, pp 417–429
- Bloos G, Dietl G, Schweigert G (2006) Der Jura Süddeutschlands in der Stratigraphischen Tabelle von Deutschland 2002. *Newsl Stratigr* 41(1–3):263–277. <https://doi.org/10.1127/0078-0421/2005/0041-0263>
- Chu V, Regev L, Weiner S, Boaretto E (2008) Differentiating between anthropogenic calcite in plaster, ash and natural calcite using infrared spectroscopy: implications in archaeology. *J Archaeol Sci* 35(4):905–911. <https://doi.org/10.1016/j.jas.2007.06.024>
- Cuomo di Caprio N (1972) Proposta di classificazione delle fornaci per ceramica e laterizi nell'area italiana. *Sibrium* 11:371–464
- Cuomo di Caprio N (2007) *Ceramica in Archeologia*. L'Erma Bretschneider, Roma
- Delcroix G, Huot JL (1972) Les fours dits “de potier” dans l'Orient ancien. *Syria* 49(1–2):35–95
- Dufay, B (1996) Les fours de potiers gallo-romains : synthèse et classification. Un nouveau panorama. Actes du congrès de la Société Française de l'Etude de la Céramique Antique en Gaule, (Dijon, 16–19 May 1996), p 297–312
- Duhamel P (1974) Les fours de potiers. *Dossiers de l'archéologie* 6:54–66
- Fabbri B, Gualtieri S, Shoval S (2014) The presence of calcite in archaeological ceramics. *J Eur Ceram Soc* 34(7):1899–1911. <https://doi.org/10.1016/j.jeurceramsoc.2014.01.007>
- Forget MCL, Regev L, Friesem DE, Shahack-Gross R (2015) Physical and mineralogical properties of experimentally heated chaff-tempered mud bricks: implications for reconstruction of environmental factors influencing the appearance of mud bricks in archaeological conflagration events. *J Archaeol Sci Rep* 2:80–93. <https://doi.org/10.1016/j.jasrep.2015.01.008>
- Friesem DE, Tsartsidou G, Karkanias P, Shahack-Gross R (2014) Where are the roofs? A geo-ethnoarchaeological study of mud brick structures and their collapse processes, focusing on the identification of roofs. *Archaeol Anthropol Sci* 6:73–92. <https://doi.org/10.1007/s12520-013-0146-3>
- Gibbs K (2015) Pottery invention and innovation in East Asia and the Near East. *Camb Archaeol J* 25(1):339–351. <https://doi.org/10.1017/S0959774314001139>
- Gibson AM, Woods AJ (1990) *Pottery for the archaeologist*. Columbia University Press, New-York
- Gliozzo E (2020) Ceramic technology. How to reconstruct the firing process. *Archaeol Anthropol Sci* 12:260. <https://doi.org/10.1007/s12520-020-01133-y>

- Gosselain OP (1992) Bonfire of the enquiries. Pottery firing temperatures in archaeology: What for? *J Archaeol Sci* 19(3):243–259. [https://doi.org/10.1016/0305-4403\(92\)90014-T](https://doi.org/10.1016/0305-4403(92)90014-T)
- Hanning E, Döhner G, Grunwald L, Hastenteufel A, Rech A, Axtmann A, Bogott A (2016) Experimental reconstruction and firing of a 5/6th century updraft kiln from Mayen, Germany. *Experimentelle Archäologie Europa* 15:60–73
- Hansen Streily A (2000) Early pottery kilns in the Middle East. *Paléorient* 26(2):69–81
- Hasaki E (2002) Ceramic kilns in ancient Greece: technology and organization of ceramic workshops. PhD thesis, University of Cincinnati
- Heimann RB, Maggetti M (2019) The struggle between thermodynamics and kinetics: phase evolution of ancient and historical ceramics. In: Artioli G, Oberti R (eds) *The contribution of mineralogy to cultural heritage. The European Mineralogical Union and the Mineralogical Society of Great Britain and Ireland*, London, pp 233–281
- Helfert M, Mecking O, Lang F, von Kaenel HM (2011) Neue Perspektiven für die Keramikanalytik. Zur Evaluation der portablen energiedispersiven Röntgenfluoreszenzanalyse (P-ED-RFA) als neues Verfahren für die geochemische Analyse von Keramik in der Archäologie. *Frankfurter elektronische Rundschau zur Altertumskunde* 14:1–30
- Karkanas P (2007) Identification of lime plaster in prehistory using petrographic methods: a review and reconsideration of the data on the basis of experimental and case studies. *Geoarchaeology Int J* 22(7):775–96. <https://doi.org/10.1002/gea.20186>
- Karkanas P, Berna F, Fallu D, Gauß W (2019) Microstratigraphic and mineralogical study of a Late Bronze Age updraft pottery kiln, Kolonna Site, Aegina Island, Greece. *Archaeol Anthropol Sci* 11:5763–5780. <https://doi.org/10.1007/s12520-019-00903-7>
- Kazakou T, Zorba T, Vourlias G, Pavlidou E, Chrissafis K (2019) Combined studies for the determination of the composition and the firing temperature of ancient and contemporary ceramic artefacts. *Thermochim Acta* 682:178–412. <https://doi.org/10.1016/j.tca.2019.178412>
- Kingery WD (1997) The operational principles of ceramic kilns. In: Rice PM (ed) *Ceramics and Civilisation. Vol. VII. The Prehistory and History of Ceramic Kilns. The American Ceramic Society, Columbus*, pp 11–19
- Livingstone Smith A (2001) Bonfire II: the return of pottery firing temperatures. *J Archaeol Sci* 28(9):991–1003. <https://doi.org/10.1006/jasc.2001.0713>
- Maggetti M (1982) Phase analysis and its significance for technology and origin. In: Olin JS, Franklin AD (eds) *Archaeological ceramics. Smithsonian Institution, Washington*, pp 121–133
- Maggetti M, Neururer C, Ramseyer D (2011) Temperature evolution inside a pot during experimental surface (bonfire) firing. *Appl Clay Sci* 53(3):500–508. <https://doi.org/10.1016/j.clay.2010.09.013>
- Maniatis Y, Tite MS (1975) A scanning electron microscope examination of the bloating of fired clays. *Trans J Br Ceram Soc* 74(8):229–232
- Maniatis Y, Tite MS (1981) Technological examination of Neolithic Bronze-Age pottery from central and southeast Europe and from the Near-East. *J Archaeol Sci* 8(1):59–76. [https://doi.org/10.1016/0305-4403\(81\)90012-1](https://doi.org/10.1016/0305-4403(81)90012-1)
- Maniatis Y, Facorellis Y, Pillali A, Papanthimou-Papaefthimiou A (2002) Firing temperature determinations of low fired clay structures. In: Kilikoglou V, Hein A, Maniatis Y (eds) *Modern trends in scientific studies on ancient ceramics. BAR International Series 1011. Archaeopress, Oxford*, pp 59–68
- van der Marel HW, Beutelspacher H (1976) *Atlas of infrared spectroscopy of clay minerals and their admixtures. Elsevier Scientific, Amsterdam*
- Margenot AJ, Calderón FJ, Goyno KW, Mukome FND, Parikh SJ (2017) IR spectroscopy, soil analysis applications. In: Lindon JC, Tranter GE, Koppenaal DW (eds) *The Encyclopedia of Spectroscopy and Spectrometry, vol 2, 3rd edn. Oxford University Press, Oxford*, pp 448–454. <https://doi.org/10.1016/B978-0-12-409547-2.12170-5>
- Maritan L, Nodari L, Mazzoli C, Milano A, Russo U (2006) Influence of firing conditions on ceramic products: experimental study on clay rich in organic matter. *Appl Clay Sci* 31(1–2):1–15. <https://doi.org/10.1016/j.clay.2005.08.007>
- Maritan L, Mazzoli C, Freestone IC (2007) Modelling changes in mollusc shell internal micro-structure during firing: implication for temperature estimate in shell-bearing pottery. *Archaeometry* 49:529–541. <https://doi.org/10.1111/j.1475-4754.2007.00318.x>
- McDonnell JG (2001) Pyrotechnology. In: Brothwell DR, Pollard AM (eds) *Handbook of Archaeological Science. Wiley, London*, pp 493–506
- Mentesana R, Kilikoglou V, Todaro S, Day PM (2019) Reconstructing change in firing technology during the final Neolithic-Early Bronze Age transition in Phaistos, Crete. Just the tip of the iceberg? *Archaeol Anthropol Sci* 11:871–894. <https://doi.org/10.1007/s12520-017-0572-8>
- Moore DM, Reynolds RC Jr (1997) *X-ray diffraction and the identification and analysis of clay minerals, 2nd edn. Oxford University Press, Oxford*
- Nodari L, Marcuz E, Maritan L, Mazzoli C, Russo U (2007) Hematite nucleation and growth in the firing of carbonate-rich clay for pottery production. *J Eur Ceram Soc* 27(16):4665–4673. <https://doi.org/10.1016/j.jeurceramsoc.2007.03.031>
- Quinn PS (2013) *Ceramic petrography. The interpretation of archaeological pottery and related artefacts in thin section. Archaeopress, Oxford*
- Quinn PS, Benzonelli A (2018) XRD and materials analysis. In: Lopez Varela S (ed) *The Encyclopedia of Archaeological Sciences. Wiley, New York*, pp 1796–1800. <https://doi.org/10.1002/9781119188230.saseas0619>
- Regev L, Poduska KM, Addadi L, Weiner S, Boaretto E (2010) Distinguishing between calcites formed by different mechanisms using infrared spectrometry: archaeological applications. *J Archaeol Sci* 37(12):3022–3029. <https://doi.org/10.1016/j.jas.2010.06.027>
- Rice PM (2015) *Pottery analysis: a sourcebook. University of Chicago Press, Chicago*
- Rogier M (2018) Scientific profit through daily routine. *EXARC.net. https://exarc.net/issue-2018-3/at/scientific-profit-through-daily-routine*. Accessed 26 August 2022
- Roux V (2019) *Ceramics and society: a technological approach to archaeological assemblages. Springer, Cham*
- Rye OS (1981) *Pottery technology. Taraxacum, Washington*
- Schedl B (2014) *Der Plan von St. Gallen. Ein Modell europäischer Klosterkultur. Böhlau, Wien*
- Shoval S, Beck P (2005) Thermo-FTIR spectroscopy analysis as a method of characterizing ancient ceramic technology. *J Therm Anal Calorim* 82(3):609–616. <https://doi.org/10.1007/s10973-005-0941-x>
- Sillar B (2007) Dung by preference: the choice of fuel as an example of how Andean pottery production is embedded within wider technical, social, and economic practices. *Archaeometry* 42(1):43–46. <https://doi.org/10.1111/j.1475-4754.2000.tb00865.x>
- Squitieri A, Amicone S, Dinckal A, Müller CE, Rohde J, Pietsch S, Herr J-J, Gur-Arieh S, Altaweel M (2022) A multi-approach study of a chalcolithic kiln in the Bora Plain (Iraqi Kurdistan): the evidence from excavation, micromorphological and pyrotechnological analyses. *Open Archaeol. https://doi.org/10.1515/opar-2022-0265*
- Swan VG (1984) *The pottery kilns of Roman Britain. Royal Commission on Historical Monuments, vol 5. Oxbow, Oxford*

- Thér R (2014) Identification of pottery firing structures using the thermal characteristics of firing. *Archaeometry* 56(S1):78–99. <https://doi.org/10.1111/arc.12052>
- Thér R, Kallistová A, Svoboda Z, Května P, Lisá L, Burgert P, Bajer A (2019) How was Neolithic pottery fired? An exploration of the effects of firing dynamics on ceramic products. *J Archaeol Method Theory* 26(3):1143–1175. <https://doi.org/10.1007/s10816-018-9407-x>
- Tite MS, (1995) Firing temperatures determination: how and why? In: Lindhal A, Stilborg O (eds) *The aim of laboratory analysis in archaeology*. KVHAA Konferenser 34, Stockholm, pp 37–42
- Tite MS, Maniatis Y (1975a) Scanning electron microscopy of fired calcareous clays. *Trans J Br Ceram Soc* 74(1):19–22
- Tite MS, Maniatis Y (1975b) Examination of ancient pottery using the scanning electron microscope. *Nature* 257:122–123. <https://doi.org/10.1038/257122a0>
- Toffolo MB, Boaretto E (2014) Nucleation of aragonite upon carbonation of calcium oxide and calcium hydroxide at ambient temperatures and pressures: a new indicator of fire-related human activities. *J Archaeol Sci* 49:237–248. <https://doi.org/10.1016/j.jas.2014.05.020>
- Tremp E (2014) *Der St. Galler Klosterplan (Begleittext)*. In: Stiftsbibliothek St. Gallen (ed) *Der St. Galler Klosterplan*. Faksimile, Begleittext, Beischriften und Übersetzung. Verlag am Klosterhof, St.Gallen
- Weiner S (2010) *Microarchaeology: beyond the visible archaeological record*. Cambridge University Press, Cambridge
- Weiner S, Nagorsky A, Taxel I, Asscher Y, Albert RM, Regev L, Yan X, Natalio F, Boaretto E (2020) High temperature pyrotechnology: a macro- and microarchaeology study of a late Byzantine-beginning of Early Islamic period (7th century CE) pottery kiln from Tel Qatra/Gedera, Israel. *J Archaeol Sci Rep* 31:102–263. <https://doi.org/10.1016/j.jasrep.2020.102263>
- Wertime TA (1964) Man's first encounters with metallurgy. *Science* 146(3649):1257–1267. <https://doi.org/10.1126/science.146.3649.1257>
- Whitbread IK (1995) *Greek transport amphorae: a petrological and archaeological study*. British School at Athens, Athens
- Whitney DL, Evans BW (2010) Abbreviations for names of rock forming minerals. *Am Miner* 95:185–187

**Publisher's note** Springer Nature remains neutral with regard to jurisdictional claims in published maps and institutional affiliations.